Royal Netherlands Meteorological Institute
Ministry of Infrastructure and Water Management

The EUMETSAT Network of Satellite Application Facilities

OSI SAF
Ocean and Sea Ice

EUMETSAT

Ocean and Sea Ice SAF

An improved 2DVAR batch grid

SAF/OSI/CDOP3/KNMI/TEC/TN/339

18 February 2019

Jur Vogelzang

Royal Netherlands Meteorological Institute (KNMI)
De Bilt, the Netherlands

DOCUMENTATION CHANGE RECORD

Reference: SAF/OSI/KNMI/TEC/TN/339

Issue / Revision :	Date :	Change :	Description :
Version 0.1	2017-09-08		1st draft by Jur Vogelzang
Version 0.2	2019-01-10	Review	By Ad Stoffelen
Version 1.0	2019-02-18	Some additions	By Jur Vogelzang

Summary

Two-dimensional variational ambiguity removal (2DVAR) is the default ambiguity removal method in the KNMI wind processors AWDP and PenWP. Between October 2017 and April 2018 a new version of 2DVAR was developed and validated. This report describes the improvements made to 2DVAR and their effect on the resulting 2DVAR wind fields.

The new 2DVAR differs from the old one in the following aspects: the 2DVAR grid is as regular as possible, and the interpolation of irregularly spaced observations in the 2DVAR grid is considerably improved.

The 2DVAR grid is constructed for each batch from the coordinates of the batch grid cells and spherical trigonometry. The interpolation of observations in the 2DVAR grid is done in 3D using simple vector algebra. Buoy comparison indicates that the improved interpolation procedure has most effect.

The new 2DVAR winds compare slightly better with buoy winds for ASCAT-5.6, while the effect is neutral for the other ASCAT products. Some selected cases suggest a positive effect for all ASCAT products.

Contents

1 Introduction

1.1 Problem formulation

Two-dimensional Variational Ambiguity Removal (2DVAR) is the default ambiguity removal method in the wind processors developed at KNMI. 2DVAR constructs a 2D meteorological analysis from the ambiguous wind solutions and an NWP forecast as background field, and then selects the ambiguity closest to the analysis as preferred solution.

2DVAR is very similar to the 3DVAR and 4DVAR data assimilation systems used in NWP. The analysis increments are calculated by minimizing a cost function consisting of an observation part and a background part. The minimization is done in Fourier space, because this reduces the dimensionality of the background cost function calculation by a factor of two (provided that the background error correlation is a function of distance only [*Vogelzang and Stoffelen*, 2018]). A prerequisite is that the analysis increments are defined on a regular grid named the 2DVAR grid. In the past versions of the ASCAT Wind Data Processor, AWDP-2.4, and the Pencil Beam Wind Processor (PenWP-2.1) the 2DVAR grid is taken as a subset of the observation grid (WVC grid) with a stride between 4 and 8. Since the analysis increments are calculated in the Fourier domain, the 2DVAR grid must be extended in all directions in order to let the increments go close to zero at the edges of the 2DVAR grid. The size of the extension depends on the type of background error correlation used. It is 1800 km for Gaussian error correlations and 6000 km for empirical ones. This makes the 2DVAR grid quite large, so its grid size is taken a factor 4 to 8 larger than the WVC grid size for computational efficiency. Moreover, the analysis should be just precise enough to select the correct ambiguity. The analysis increments at the position of the observations, needed to calculate the observation part of the cost function, are obtained by bilinear interpolation.

The 2DVAR grid is thus constructed from the WVC grid with the tacit assumption that the WVC grid is regular, so the interpolation coefficients of observations in the 2DVAR grid are inverse integers. This assumption does not hold for ASCAT-coastal and ASCAT-6.25, since WVCs near the coast may be shifted seaward when calculating the average radar cross sections from the full resolution data. As a result, their contribution to the observation cost function is based on an analysis increment evaluated at the wrong position. For the ASCAT-5.6 product the radar cross sections are calculated using an optimized antenna footprint pattern. As a consequence, it comes on a WVC grid with varying size in the cross-track direction.

In the future coastal products from other scatterometers may become available. Reprocessing these with 2DVAR as ambiguity removal method requires software to construct a regular 2DVAR grid from an irregular WVC grid.

1.2 Aims and scope

The aim of this study is to extend AWDP and PenWP with software to calculate a regular 2DVAR grid from the input and to implement a simple and effective interpolation method for irregularly spaced observations in the 2DVAR grid.

1.3 Introductory remarks

In chapter 2 we present a simple and effective method to construct a regular 2DVAR grid for each batch separately and a simple interpolation method for irregularly spaced observations into the 2DVAR grid.

Chapter 3 contains comparisons with buoy winds of ASCAT-coastal, ASCAT-6.25, and ASCAT-5.6 processed from full resolution L1B data. The buoy comparisons show a slight improvement for ASCAT-5.6 and a neutral effect for the two other products, though some selected cases show improvements for all grid sizes.

Chapter 4 considers the general case in which only BUFR data on a possibly irregular grid are available. Buoy comparison shows no significant effect, as expected.

The conclusions are given in chapter 5.

2 New 2DVAR

2.1 Construction of the 2DVAR grid

The 2DVAR grid may be constructed from the positions of the observations within a batch as follows:

1. Find the coordinates of point 1, the center of the first row of the batch.
2. Find the coordinates of point *n*, the center of the last point of the batch.
3. Define a great circle through points 1 and *n*. This is the "backbone" of the 2DVAR grid.
4. Go along the backbone, starting well before point 1 and ending well beyond point *n* in order to incorporate the 2DVAR buffer zone, with steps equal to the 2DVAR grid size. For each point on the backbone, find the direction of the normal to the backbone (the "rib") as the direction between the current backbone point and point *p*. Define the 2DVAR grid points along the rib using the rib direction and the required distance from the backbone.

One can also visualize the procedure as the backbone being the equator and the ribs being meridians which all meet at the poles.

In steps 1 and 2, it is not necessary to have the coordinates of the first and last point of the first or last row; in between points can also do the job, because points 1 and *n* need not be known very precise. However, in order to simplify the code in case the two ASCAT swaths are processed in one batch, it is required that the first point has a WVC index between 1 and *N*/2 and the last point a WVC index between *N*/2+1 and *N*, where *N* is the number of WVCs in the batch. Also, it is not necessary that point 1 is found in the first row of the batch and point *n* in the last row. Other rows are usable too, as long as the appropriate 2DVAR buffer is retained in step 4.

It may happen that a batch contains only one row of data. In that case no point 2 can be found, and the backbone direction is defined as normal to the data row direction. This happens for small batches only, so the precision of this procedure is sufficient.

The 2DVAR grid obtained this way is as regular as possible, since the grid points along a row lie on a great circle and the centers of the rows also lie on a great circle. The only drawback is that the 2DVAR buffer zone needs to be larger by 300 km, because the satellite ground track is *not* on a great circle (it would be if the Earth stood still). However, it turns out that the maximum distance between the backbone of the 2DVAR grid and the ground track does not exceed ± 300 km for a batch of 1/6-th orbit long. Therefore the 2DVAR grid dimensions are slightly larger in the new 2DVAR, but the interpolation method presented in the next paragraph is greatly accommodated by the regularity of the new 2DVAR grid.

2.2 Interpolation method

Since the observations may be irregularly placed with respect to the 2DVAR grid, a new interpolation algorithm needs to be developed. The interpolation coefficients are calculated in three dimensional Euclidian space using some basic vector algebra given below. The advantage of this approach is that it is simple and works well above the poles where spherical trigonometric methods may run into problems. The disadvantage is some loss of precision, because a spherical Earth can't be exactly covered with square tiles. However, the errors involved are small.

Suppose we have a WVC with its center at geographical longitude λ and latitude φ. With the WVC center one can associate a vector $\mathbf{r}$ on the unit sphere as

$$\mathbf{r} = \begin{pmatrix} \cos\lambda \sin\varphi \\ \sin\lambda \sin\varphi \\ \cos\varphi \end{pmatrix} \quad , \tag{2.1}$$

The WVC center falls in a parallelogram with as corner points the centers of 2DVAR grid cells with indices (i, j), $(i+1, j)$, $(i, j+1)$, and $(i+1, j+1)$, with i the index in the along-track direction (row direction) and j in the cross-track direction (WVC direction), with the cross track direction to the right of the satellite heading. To each of the WVC centers one can also associate a vector on the unit sphere as given by (2.1).

Now let

$$\mathbf{a} = \mathbf{r}_{i+1,j} - \mathbf{r}_{i,j} \quad , \quad \mathbf{c} = \mathbf{r}_{i,j+1} - \mathbf{r}_{i,j} \quad , \tag{2.2}$$

be vectors in the along-track and cross-track directions, respectively. These vectors span the parallelogram which contains the WVC center. Then we can define the coefficients α and β as

$$\alpha = \frac{\mathbf{a} \cdot \mathbf{r}}{\mathbf{a} \cdot \mathbf{a}} \quad , \quad \beta = \frac{\mathbf{c} \cdot \mathbf{r}}{\mathbf{c} \cdot \mathbf{c}} \quad . \tag{2.3}$$

The bilinear interpolation of any quantity f given at the 2DVAR grid cell centers now reads

$$f = \alpha\beta f_{i+i,j+1} + \alpha(1-\beta) f_{i+1,j} + (1-\alpha)\beta f_{i,j+1} + (1-\alpha)(1-\beta) f_{i,j} \quad . \tag{2.4}$$

If both α and β are in [0,1] the WVC falls within the square spanned by the four 2DVAR grid centers. If α is smaller than zero, the index i should be reduced, and if it is larger than one, the index should be increased. Similarly, if β is smaller than zero, the index j should be reduced, and when it is larger than one the index should be increased. This gives a fast iterative algorithm to determine the correct along-track and cross-track 2DVAR indices and the corresponding interpolation coefficients for each WVC.

As noted above, the figure spanned by the four 2DVAR grid cell centers is not exactly a parallelogram, since the 2DVAR grid is defined on a sphere. As a consequence, the coefficients α and/or β may hop between values smaller than zero and values larger than one during iteration, with

a periodicity of two (alternating), three, or higher. This is easily checked for and when it is detected the most recent values are truncated within [0,1] and returned by the algorithm.

Note that the 2DVAR grid and interpolation method are fully based on geographical coordinates. Gaps in the WVC grid due to missing radar data have therefore no longer effect on 2DVAR.

3 ASCAT from L1B

3.1 Data

All ASCAT-A data from January 2015 were reprocessed for ASCAT-coastal, ASCAT-6.25, and ASCAT-5.6, using the following processing options:

- old — old 2DVAR with default settings
- new — new 2DVAR with default settings
- new + 2s1b — new 2DVAR with both swaths processed in a single batch
- new + 2s1b + EBEC — new 2DVAR with both swaths processed in a single batch and empirical background error correlations

The ASCAT data were collocated with all buoy data not blacklisted by ECMWF. The 2DVAR grid size is 50 km for ASCAT-coastal and ASCAT-6.25, and 43.75 km (7 × 6.25 km) for ASCAT-5.6.

3.2 Buoy comparison

3.2.1 Selected wind

The results of the buoy comparison for the 2DVAR selected winds are shown in table 3.1. Table 3.1 shows the standard deviations of the differences between buoys and ASCAT for wind speed (σ_s), wind direction (σ_d), zonal wind component (σ_u), and meridional wind component (σ_v). The last column gives the number of collocations used. For each WVC grid size only common collocations were considered for intercomparison of various 2DVAR types. The number between brackets is for wind direction, since wind statistics were only calculated for wind speeds exceeding 4 m/s. The accuracy in the standard deviations is about 1.7%, leading to accuracies of 0.02 m/s in wind speed, 0.3° in wind direction, and 0.03 m/s in both zonal and meridional wind component.

WVC grid size (km)	**2DVAR type**	σ_s **(m/s)**	σ_d **(deg.)**	σ_u **(m/s)**	σ_v **(m/s)**	N
12.5 (coastal)	old	1.01	15.0	1.46	1.61	3368 (2859)
	new	1.01	14.9	1.46	1.61	3368 (2859)
	new+2s1b	1.01	14.9	1.46	1.60	3368 (2859)
	new+2s1b+EBEC	1.01	14.3	1.45	1.62	3368 (2859)
6.25	old	1.03	15.2	1.50	1.69	3311 (2802)
	new	1.03	15.2	1.50	1.68	3311 (2802)
	new+2s1b	1.03	15.2	1.50	1.69	3311 (2802)
	new+2s1b+EBEC	1.03	14.8	1.50	1.69	3311 (2801)
5.6	old	1.02	15.0	1.51	1.68	3537 (2971)
	new	1.02	14.7	1.51	1.68	3537 (2981)
	new+2s1b	1.02	14.7	1.51	1.68	3537 (2981)
	new+2s1b+EBEC	1.03	14.4	1.50	1.69	3537 (2982)

Table 3.1 Buoy comparison for 2DVAR selected wind.

For ASCAT-coastal and ASCAT-6.25 there are no significant differences in buoy comparison between the old and the new 2DVAR. For ASCAT-5.6 the new 2DVAR gives a slightly better comparison in wind direction. This is as expected, because in the old 2DVAR implementation the 2DVAR grid is irregular.

Performing 2DVAR on both swaths in a single batch has no significant effect for ASCAT-coastal, ASCAT-6.25, and ASCAT-5.6. Note that processing of both swaths in one batch was introduced mainly to reduce processing time for the ultra-high resolution products.

Use of empirical background error correlations (EBECs) in 2DVAR leads to a better buoy comparison for ASCAT-coastal, ASCAT-6.25, and ASCAT-5.6. This agrees with the results in [*Vogelzang and Stoffelen*, 2017], which is not too surprising, since that study also used the January 2015 data.

The results in table 3.1 are for all buoys not blacklisted by ECMWF. Table 3.2 contains the results for the buoy comparison with coastal buoys, i.e., buoys included in the ASCAT-coastal collocations, but not in the ASCAT-25 collocations. Table 3.2 is similar to table 3.1, except that there are, of course, no results for ASCAT-25. The number of buoys in the coastal zone is much smaller than the total number of buoys, as can be seen from the last column of table 3.2. As a consequence, the precision in the standard deviations is about 6%, yielding precisions in the standard deviations of about 0.06 m/s for wind speed, 1.0 degree for wind direction, and 0.1 m/s for the wind components.

WVC grid size (km)	**2DVAR type**	σ_s **(m/s)**	σ_d **(deg.)**	σ_u **(m/s)**	σ_v **(m/s)**	N
12.5 (coastal)	old	1.08	17	1.5	1.7	353 (294)
	new	1.08	17	1.5	1.6	353 (294)
	new+2s1b	1.08	17	1.5	1.6	353 (294)
	new+2s1b+EBEC	1.08	14	1.4	1.6	353 (294)
6.25	old	1.19	15	1.5	1.9	347 (287)
	new	1.19	15	1.5	1.9	347 (287)
	new+2s1b	1.19	15	1.5	1.9	347 (287)
	new+2s1b+EBEC	1.19	15	1.4	1.8	347 (287)
5.6	old	1.19	13	1.5	1.8	375 (311)
	new	1.18	13	1.5	1.8	375 (311)
	new+2s1b	1.18	13	1.5	1.8	375 (311)
	new+2s1b+EBEC	1.17	14	1.5	1.9	375 (311)

Table 3.2 Buoy comparison for 2DVAR selected wind in the coastal zone.

Table 3.2 shows that there are no significant differences between the various 2DVAR types for a given WVC size, except for an improvement in wind direction for ASCAT-coastal with EBECs.

Comparison with table 3.1 shows some striking differences. For ASCAT-6.25 and ASCAT-5.6 the difference in wind speed and wind component v is significantly higher in the coastal zone, while the difference in wind direction is about the same.

Note that these differences apply to both the old and the new 2DVAR, and that the standard deviation in wind speed in the coastal zone is higher for ASCAT-6.25 and ASCAT-5.6 than for ASCAT-

coastal, while in the open ocean (table 3.1) the opposite trend was found. We note several effects, such as 1) the collocated buoy set or weather sample is different for each product in each area and thus provides different statistics, 2) more variability exists near the coast due to land-sea breezes and sea currents, either generated by differential heating, wind and tides and 3) besides the collocation distance, also the position of the buoy with respect to scatterometer WVCs and land boundary affect the verification. It may be useful to further test these effects over longer periods and by single buoy data sets. Note that buoy wind measurements are with respect to the fixed earth, while the roughness measured by scatterometers is generated by relative motion between the air and the moving ocean surface.

3.2.2 Analysis

Table 3.3 shows the comparison of the 2DVAR analysis with the buoy winds. Table 3.3 is again similar to table 3.1.

WVC grid size (km)	**2DVAR type**	σ_s **(m/s)**	σ_d **(deg.)**	σ_u **(m/s)**	σ_v **(m/s)**	N
12.5 (coastal)	old	1.31	14.2	1.64	1.74	3368 (2801)
	new	1.30	14.1	1.63	1.72	3368 (2796)
	new+2s1b	1.29	14.2	1.63	1.73	3368 (2799)
	new+2s1b+EBEC	1.11	13.0	1.49	1.59	3368 (2822)
6.25	old	1.26	14.0	1.62	1.73	3311 (2723)
	new	1.26	13.9	1.62	1.73	3311 (2729)
	new+2s1b	1.26	14.1	1.62	1.73	3311 (2730)
	new+2s1b+EBEC	1.08	13.0	1.48	1.57	3311 (2759)
5.6	old	1.26	14.3	1.65	1.71	3537 (2889)
	new	1.26	13.7	1.61	1.71	3537 (2900)
	new+2s1b	1.26	14.2	1.63	1.71	3537 (2900)
	new+2s1b+EBEC	1.06	13.0	1.49	1.58	3537 (2928)

Table 3.3 Buoy comparison for 2DVAR analysis wind.

For ASCAT-coastal and ASCAT-6.25 there is no significant difference, while for ASCAT-5.6 there is an improvement in wind direction and zonal wind component u. Processing both swaths in a single batch has a slightly negative effect on wind direction for ASCAT-5.6. Use of EBECs significantly improves the quality of the 2DVAR analysis. In fact, the 2DVAR analysis in case of EBECs shows an improved buoy verification of wind direction (for slightly less samples) and meridional wind with respect to the end products, while 2DVAR wind speeds appear relatively degraded.

The positive or negative impacts of the various 2DVAR settings on the analysis in table 3.3 can be found back in table 3.1 for the selected wind, but weaker. This is because the selected wind is obtained from four ambiguities at most, and therefore a considerable change in analysis wind is needed to force selection of another ambiguity.

Table 3.4 is similar to table 3.3, but now restricted to coastal zone buoys as in table 3.2. No significant difference between the various 2DVAR types for the different ASCAT products is found, except for a significant improvement when using EBECs. Comparison with table 3.3 shows again that the analysis wind speed in the coastal zone is slightly more variable than that in the open ocean, while the analysis wind direction is somehow better (with a slightly smaller sample). Again, there may be several causes for this, such as different global sampling, that were not further elaborated.

It would also be interesting to compare the 2DVAR analysis verification with the end product verification after selection, now that the 2DVAR analysis has been much improved with EBEC, but which is not elaborated here, since only a the small data set used for this report.

WVC grid size (km)	**2DVAR type**	σ_s **(m/s)**	σ_d **(deg.)**	σ_u **(m/s)**	σ_v **(m/s)**	N
12.5 (coastal)	old	1.36	13	1.7	1.6	353 (281)
	new	1.33	13	1.6	1.6	353 (280)
	new+2s1b	1.33	13	1.6	1.6	353 (280)
	new+2s1b+EBEC	1.19	12	1.4	1.6	353 (282)
6.25	old	1.29	13	1.6	1.5	347 (273)
	new	1.29	13	1.6	1.5	347 (274)
	new+2s1b	1.28	13	1.6	1.5	347 (273)
	new+2s1b+EBEC	1.14	12	1.4	1.6	347 (281)
5.6	old	1.32	12	1.6	1.6	375 (292)
	new	1.34	12	1.6	1.5	375 (292)
	new+2s1b	1.33	12	1.6	1.5	375 (292)
	new+2s1b+EBEC	1.11	12	1.4	1.5	375 (299)

Table 3.4 Buoy comparison for 2DVAR analysis wind in the coastal zone.

3.3 Cases

3.3.1 Ambiguity removal errors January 1, 2015

Figure 3.1 shows an ASCAT-5.6 case recorded on January 1, 2015 near the east coast of Argentina, close to the mouth of the Rio de la Plata. The upper left panel of figure 3.1 shows the old 2DVAR selected wind overlaid on the MLE. The upper right panel shows the same for the new 2DVAR selected wind. Orange wind vectors have the KNMI QC flag set, purple wind vectors have the VarQC flag set, while unflagged winds are shown in blue. Blue background colors indicate large negative MLE values; red colors large positive MLE values.

The region is characterized by frontal activity. A southward flow in the upper part of figure 3.1 hits a westward flow in the middle and lower parts. The frontal area is visible as some WVCs with large negative MLE values and a number of VarQC flagged wind vectors.

With the new 2DVAR the frontal zone is shifted slightly to the south, leading to less VarQC flagging, hence better consistency between the 2DVAR selected wind and the ECMWF background.

The most prominent changes are in the lower part of figure 3.1 where the westward flow turns southward. The old 2DVAR selected wind field contains a lot of ambiguity removal errors in the lower central part of figure 3.1 where the wind is erroneously directed to the northeast. These errors are resolved with the new 2DVAR.

Comparing the analysis wind fields shows that the front in the upper part of figure 3.1 is located slightly more southward in the new 2DVAR analysis (lower right panel) than in the old one (lower left panel). The new 2DVAR also generated a cyclone in the upper left part of the image. The old 2DVAR analysis wind is directed towards the northwest in the central part of the image, while the new 2DVAR analysis wind is directed towards the west there. The old 2DVAR analysis has an irregularity in the lower central part which is absent in the new 2DVAR. As a result, the new 2DVAR yields a much smoother analysis wind field in the lower part of figure 3.1.

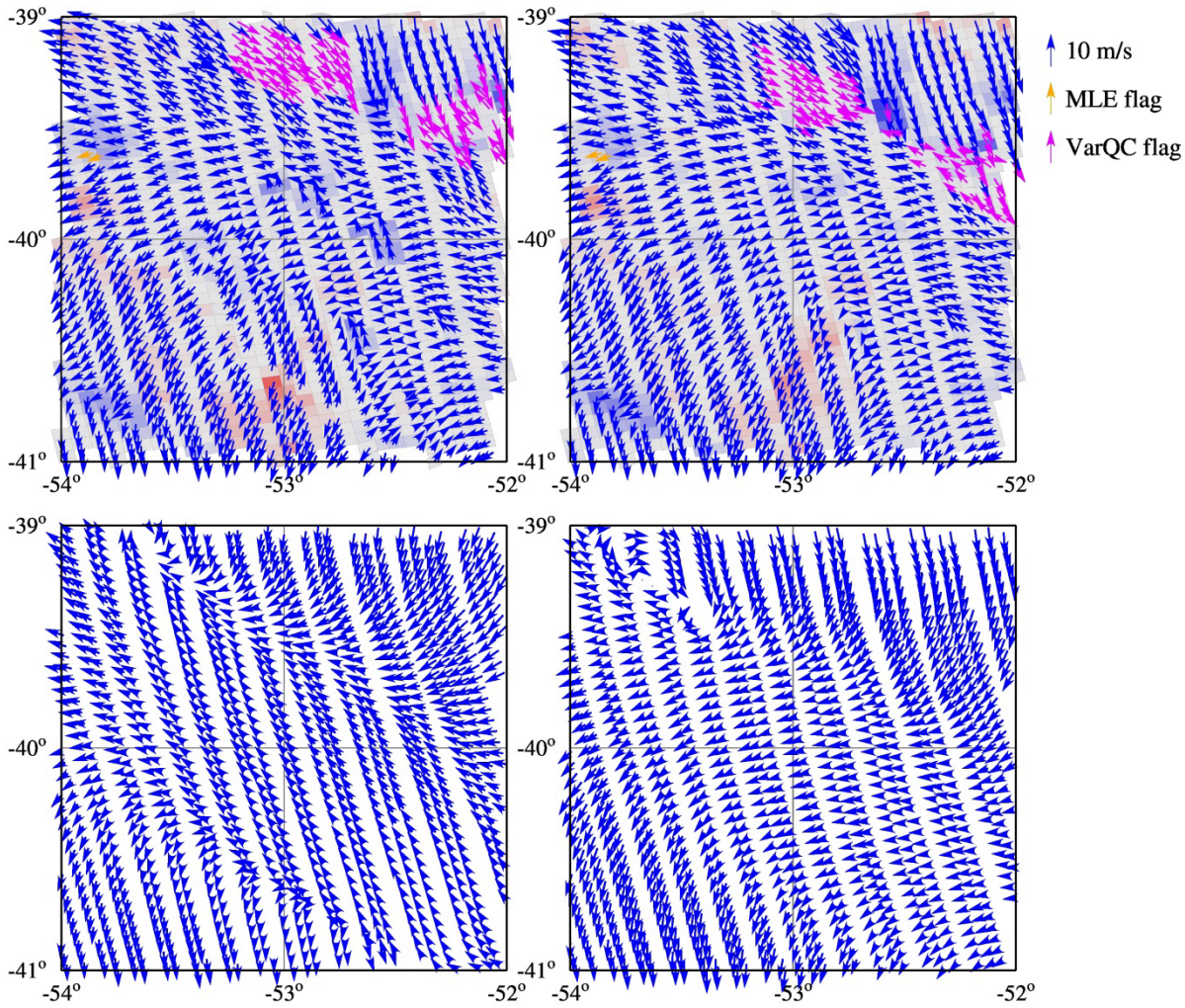

Figure 3.1 ASCAT-5.6 on January 1, 2015. Upper left: old 2DVAR selected wind overlaid on MLE; upper right: new 2DVAR selected wind overlaid on MLE; lower left: old 2DVAR analysis; lower right: new 2DVAR analysis.

Figure 3.2 is similar to figure 3.1, but for ASCAT-6.25. Also here the new 2DVAR removes the ambiguity removal errors in the lower part of the scene, though the old 2DVAR produces less errors in ASCAT-6.25 than in ASCAT-5.6. Apparently, the fact that the old 2DVAR does not account for the irregular spacing of the observations in the 2DVAR grid leads to more ambiguity removal errors in ASCAT-5.6.

The analysis wind fields of figures 3.1 and 3.2 are very similar, though the irregularity in the old 2DVAR analysis at 5.6 km is not present in the 6.25 km product. Apparently, this irregularity also results from erroneous interpolation of the observations to the 2DVAR grid.

Finally, figure 3.3 shows the same results for ASCAT-coastal. The effect of the new 2DVAR on selected wind and analysis is similar as for ASCAT-6.25 and ASCAT-5.6, though the effects are less pronounced.

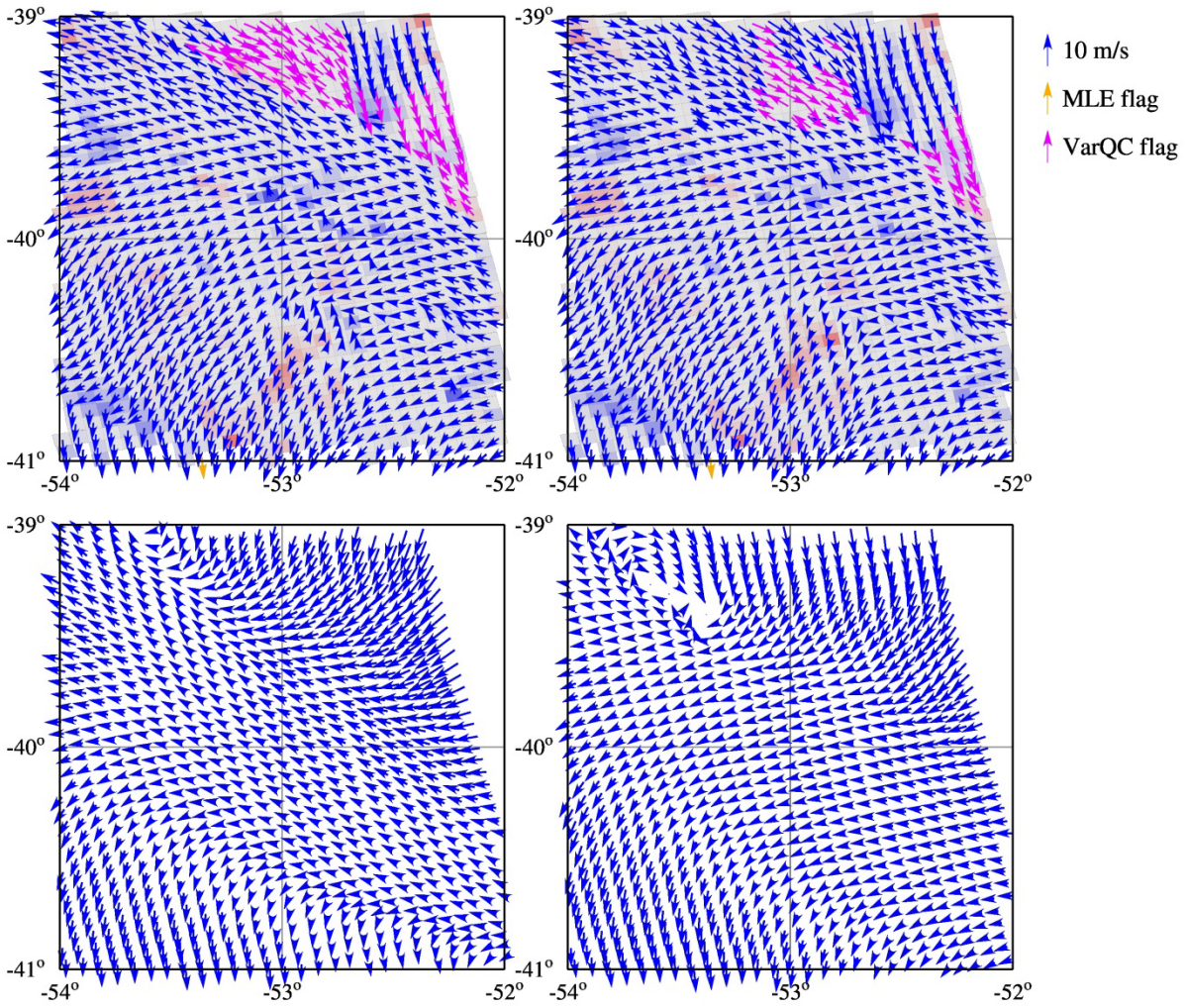

Figure 3.2 As figure 3.1, but for ASCAT-6.25.

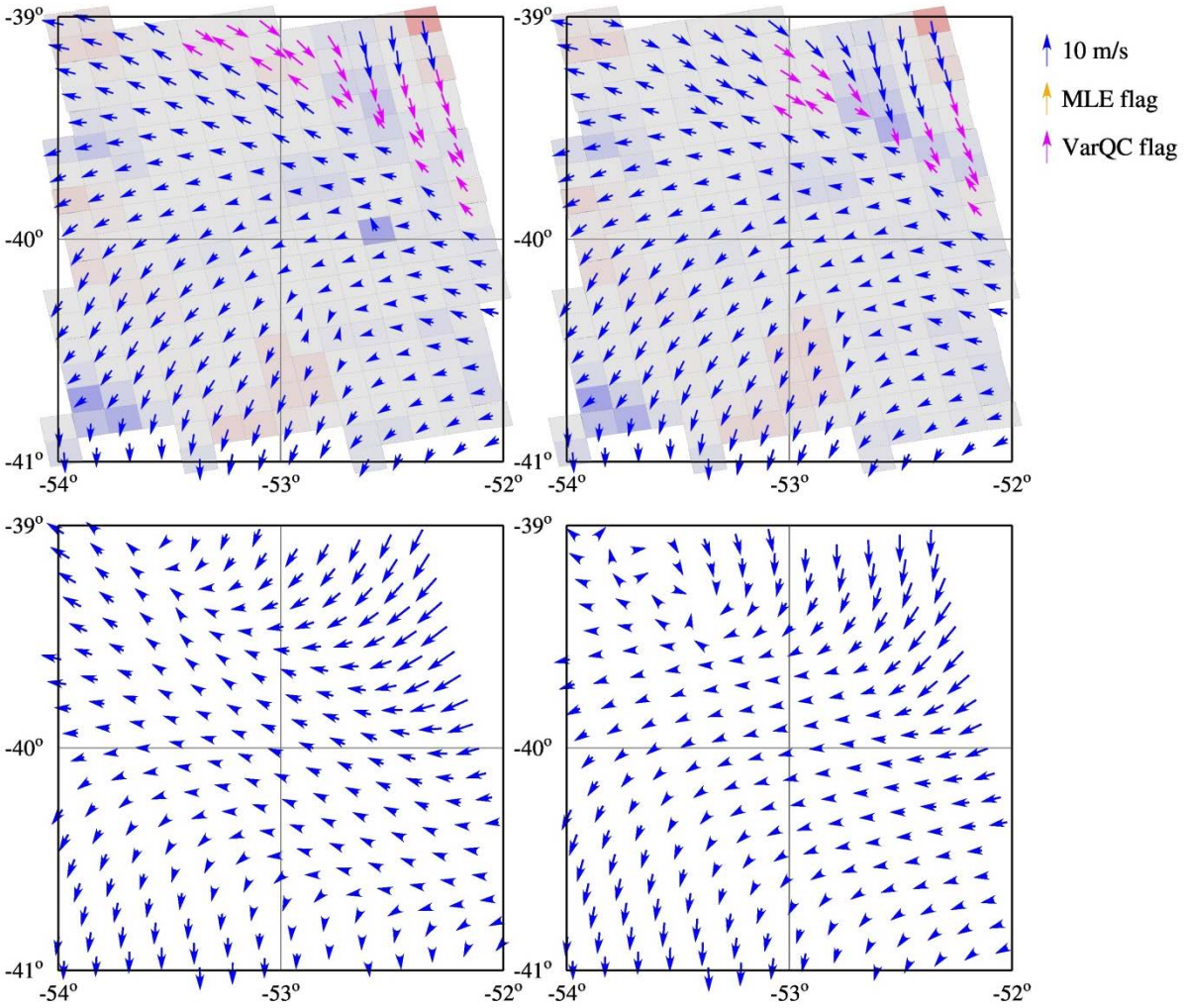

Figure 3.3 As figure 3.1, but for ASCAT-coastal.

3.3.2 Marginal ice zone January 1, 2015 (summer)

Figure 3.4 shows an ASCAT-coastal scene recorded January 1, 2015 covering the southernmost of the South sandwich Isles (visible as blank spots west of -26 °E) and the Antarctic ice edge that forms the southern boundary of the wind field. Figure 3.4 is similar to figure 3.3. The wind field selected by the old 2DVAR (upper left panel) is directed southward at the lower end of the panel, with a number of VarQC flags set. With the new 2DVAR (upper right panel) the wind is directed eastward there and in better agreement with the background. The analyses (bottom panels) show a similar behavior. The region is characterized by high negative MLE values, blue background colors in the upper panels of figure 3.4, leading to some setting of the KNMI QC flag (orange arrows).

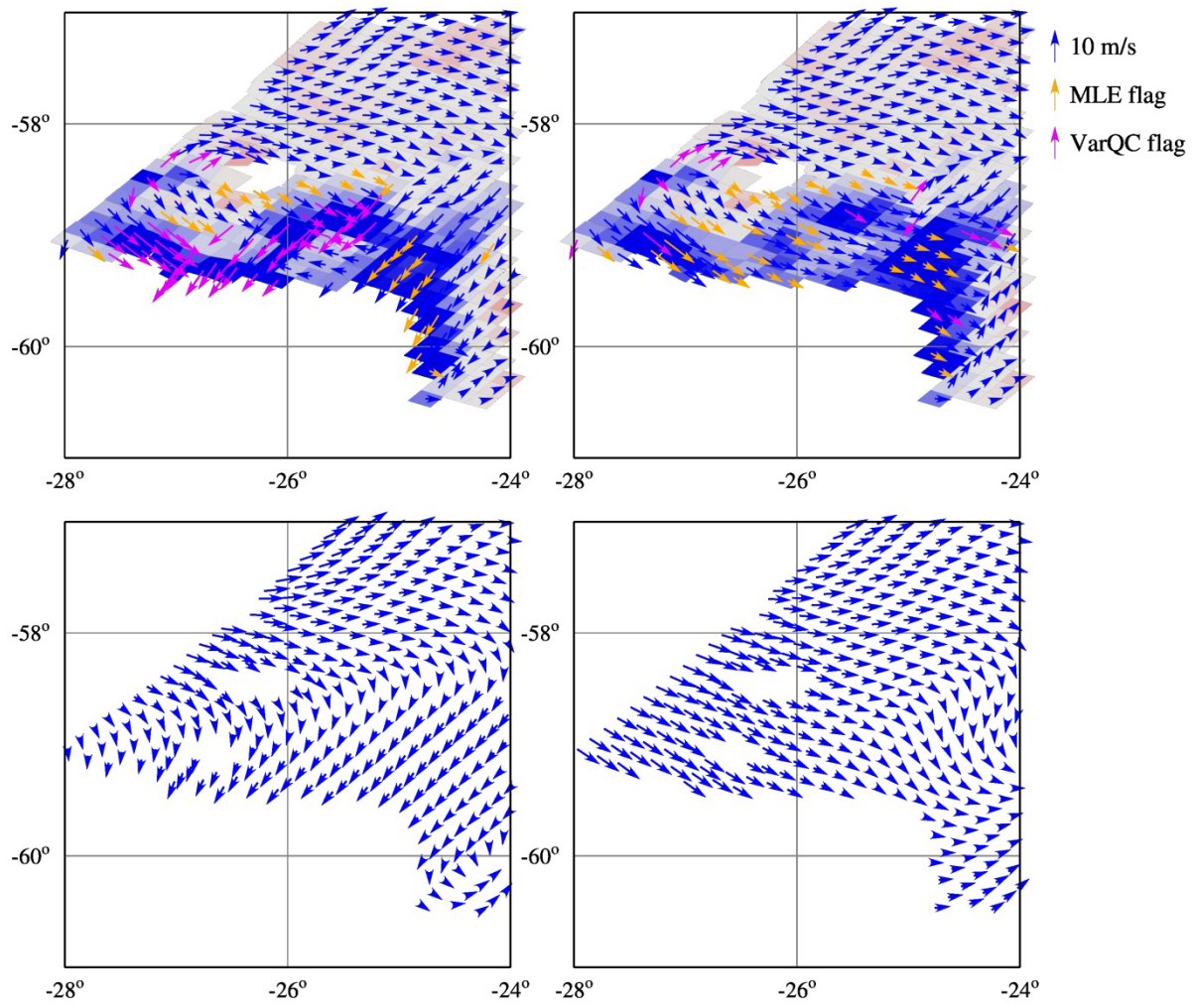

Figure 3.4 ASCAT-coastal scene recorded January 1, 2015 near the South Sandwich Isles.

Figure 3.5 shows the central area, now with ASCAT-6.25. Note that with the old 2DVAR the analysis wind direction north of the Antarctic ice edge is to the east, whereas in figure 3.4 it is towards the south. With the new 2DVAR, the analysis wind patterns of figures 3.4 and 3.5 are much more consistent. Figure 3.6 shows the ASCAT-6.25 wind field obtained with the old 2DVAR overlaid on the number of ambiguities. The number of ambiguities is set by the inversion part of the AWDP and is not affected by the ambiguity removal scheme. Note the large regions with 4 ambiguities (darkest green). For ASCAT-5.6 similar results as for ASCAT-6.25 are obtained (no results shown).

Note that the ice edge in figure 3.5 appears more southward than in figure 3.4. This is because figure 3.4 is processed with the Bayesian ice model, while figure 3.5 uses only SST as ice mask, which result in more conservative ice screening.

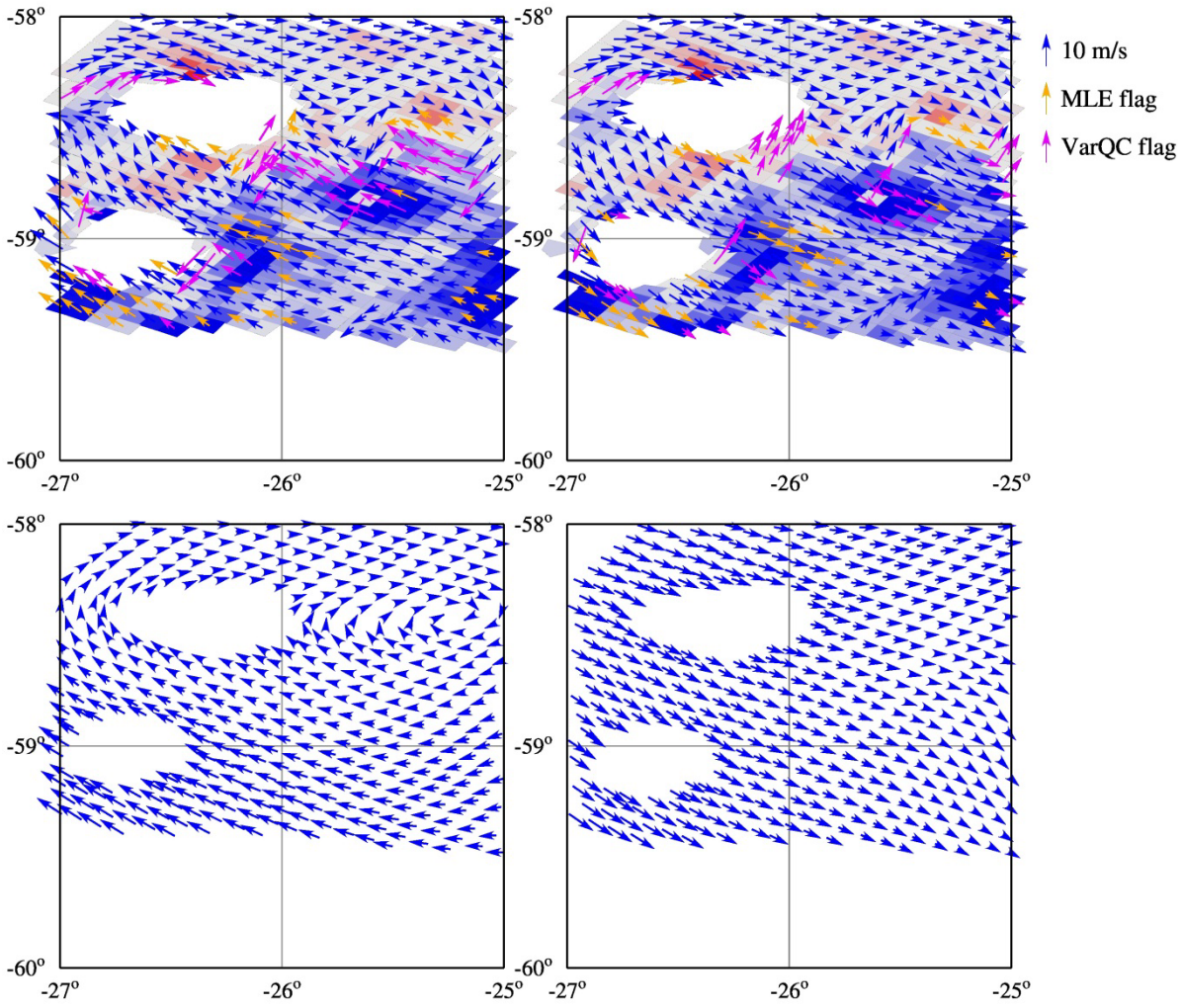

Figure 3.5 Central part of figure 3.4 with ASCAT-6.25.

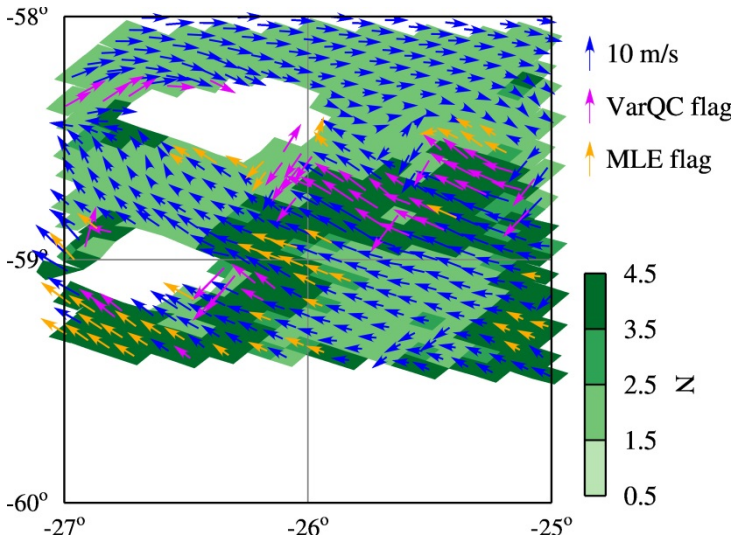

Figure 3.6 ASCAT-6.25 wind field overlaid on number of ambiguities.

3.3.3 New Zealand coastal zone January 3, 2015

Figure 3.7 shows an ASCAT-coastal scene recorded January 3, 2015 near the southern coast of New Zealand's South Island (upper) and Steward Island (right). The wind field obtained with the old 2DVAR (upper left panel) shows a westward flow between the Sothern Island and Steward Island, with some VarQC flagged WVCs. With the new 2DVAR (upper right panel) the flow is eastward everywhere. The old and new 2DVAR analyses (bottom left and bottom right panels, respectively) show a similar behavior.

ASCAT-6.25 (figure 3.8) and ASCAT-5.6 (no result shown) give similar results.

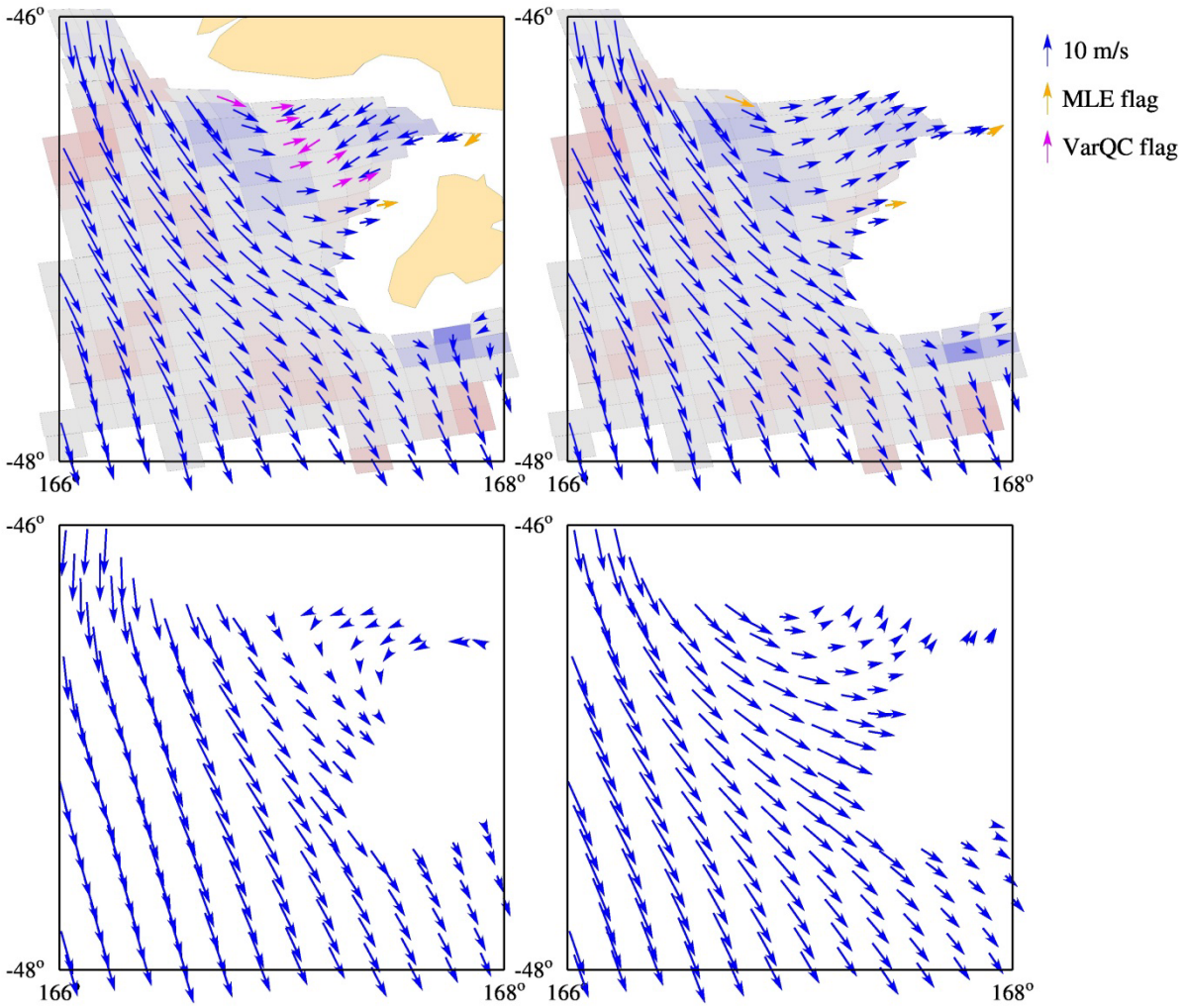

Figure 3.7 ASCAT-coastal scene south of New Zealand recorded January 3, 2015.

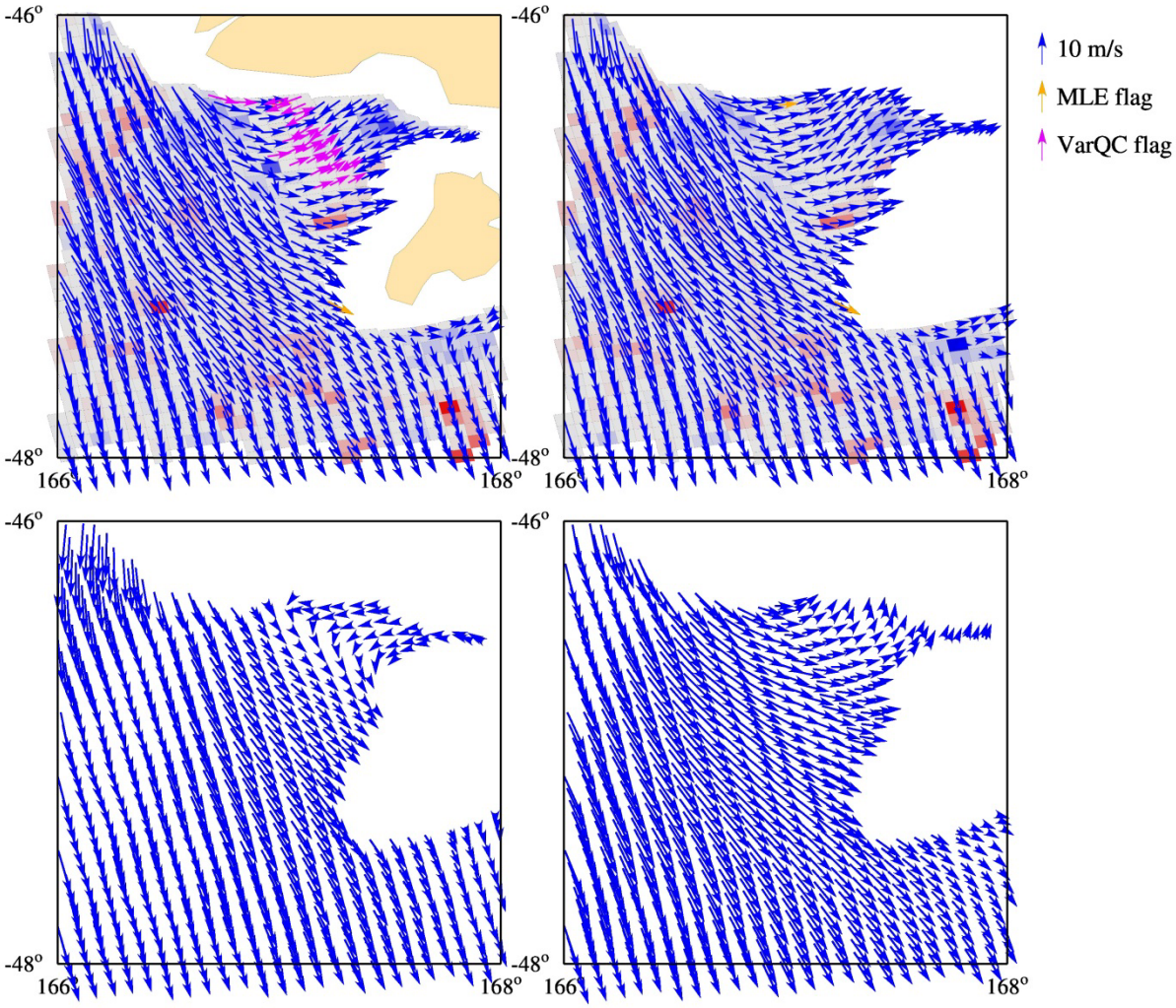

Figure 3.8 As figure 3.6, but for ASCAT-6.25.

4 ASCAT from BUFR

4.1 Data

Besides the processing mentioned in section 3.1, all ASCAT-A data from January 2015 were reprocessed for ASCAT-coastal, ASCAT-6.25, and ASCAT-5.6 without storing the analysis in the BUFR files (no `-research` option). These data sets were subsequently used as L2B input data to redo 2DVAR with default settings. Further, ASCAT-25 was also reprocessed using the following processing options:

- new + 2s1b — new 2DVAR with both swaths processed in a single batch
- new + 2s1b + EBEC — new 2DVAR with both swaths processed in a single batch and empirical background error correlations

The ASCAT data were collocated with all buoy data not blacklisted by ECMWF. The 2DVAR grid size is 100 km for ASCAT-25, 50 km for ASCAT-coastal and ASCAT-6.25, and 43.75 km (7 × 6.25 km) for ASCAT-5.6.

4.2 Buoy comparison

4.2.1 L1B and L2A

Table 4.1 shows the results of the buoy comparisons, in a way similar to that in tables 3.1 to 3.4. Table 4.1 shows no significant differences between the results obtained from L1B (labeled L1) and those obtained from L2B (labeled L2). This is as expected, since the 2DVAR grid will be very similar in both cases. Only round-off errors caused by BUFR encoding and decoding in the L2A input will induce some small changes.

WVC grid size (km)	**Input type**	σ_s **(m/s)**	σ_d **(deg.)**	σ_u **(m/s)**	σ_v **(m/s)**	N
12.5 (coastal)	L1	1.01	14.9	1.46	1.61	3371 (2862)
	L2	1.01	14.9	1.47	1.61	3371 (2862)
6.25	L1	1.03	15.2	1.50	1.68	3315 (2806)
	L2	1.03	15.2	1.50	1.68	3315 (2806)
5.6	L1	1.02	14.7	1.51	1.68	3544 (2987)
	L2	1.02	14.7	1.51	1.69	3544 (2987)

Table 4.1 Buoy comparison for 2DVAR selected wind.

Table 4.2 shows the differences between the buoy winds and the 2DVAR analysis winds for the new 2DVAR with input from L1B and input from L2B. Again, no significant differences are found.

WVC grid size (km)	Input type	σ_s (m/s)	σ_d (deg.)	σ_u (m/s)	σ_v (m/s)	N
12.5 (coastal)	L1B	1.30	14.1	1.63	1.72	3371 (2799)
	L2B	1.30	14.1	1.63	1.72	3371 (2799)
6.25	L1B	1,26	13.9	1.62	1.73	3315 (2733)
	L2B	1.26	14.0	1.62	1.73	3315 (2733)
5.6	L1B	1.27	13.7	1.60	1.71	3544 (2906)
	L2B	1.27	13.7	1.60	1.71	3544 (2906)

Table 4.2 Buoy comparison for 2DVAR analysis wind.

4.2.2 ASCAT-25

Table 4.3 shows the buoy comparison of the 2DVAR selected wind for ASCAT-25 under the various processing options. The table shows no significant differences between the various types of ASCAT-25 wind product, though the new 2DVAR seems to perform slightly worse than the old one.

2DVAR type	σ_s (m/s)	σ_d (deg.)	σ_u (m/s)	σ_v (m/s)	N
old	1.03	14.3	1.47	1.60	2870 (2457)
new	1.03	14.5	1.50	1.62	2870 (2457)
new+2s1b	1.03	14.5	1.49	1.62	2870 (2457)
new+2s1b+EBEC	1.04	14.4	1.47	1.60	2870 (2457)

Table 4.3 Buoy comparison for 2DVAR selected wind for ASCAT-25 under various processing options.

Table 4.4 shows the buoy comparison of the 2DVAR analysis wind. Without EBECs the results show no significant differences, indicating that the differences in table 4.3 between the old and the new 2DVAR are indeed insignificant. Inclusion of EBECs in 2DVAR significantly improves the analysis, but this has little effect on the selection in this sample.

2DVAR type	σ_s (m/s)	σ_d (deg.)	σ_u (m/s)	σ_v (m/s)	N
old	1.27	14.5	1.62	1.74	2870 (2414)
new	1.27	14.5	1.62	1.75	2870 (2418)
new+2s1b	1.27	14.8	1.62	1.75	2870 (2418)
new+2s1b+EBEC	1.18	14.0	1.53	1.65	2870 (2420)

Table 4.4 Buoy comparison for 2DVAR analysis wind for ASCAT-25 under various processing options.

4.3 Difference statistics

The results from the previous sections indicate that it makes little difference for the new 2DVAR whether AWDP is run with L2B input or L1B input. Table 4.5 gives the number of times a change in the 2DVAR selection index is found for the first 20 orbits of January 2015, together with the number of WVCs with a valid selection index (between 1 and 4) and the frequency with which changes in selection index occur.

WVC grid size (km)	valid WVCs	change in selection	fraction
12.5	2912255	492	$1.69\ 10^{-4}$
6.25	11403722	4998	$4.38\ 10^{-4}$
5.6	15064966	5328	$3.54\ 10^{-4}$

Table 4.5 Difference statistics for selection index.

Table 4.5 shows that the number of changes in selection index increases with decreasing WVC grid size. Note that the frequency of changes is lower for ASCAT-5.6 than for ASCAT-6.25. This may be attributed to the better radiometric stability of ASCAT-5.6. Nevertheless, the order of magnitude of the frequency of changes in selection index is the same for all three products.

Not all BUFR files were included when calculating the changes in selection index: the files recorded on January 1 at 07:00 and 17:03 and the file recorded on January 2 at 08:18 were discarded. This is because a transponder field campaign was held in this period, and therefore no full resolution data are available during the overpasses over the transponder. When processed from full resolution data, the ASCAT-5.6 BUFR file contains a considerable section without data; when reprocessed from L2B BUFR data, these missing parts are filtered out. As a result, the BUFR files have unequal length and cannot be compared easily.

5 Conclusions

In this report a new 2DVAR is proposed and tested on one month of ASCAT data. The new 2DVAR has two main advantages over the old one:

1. The new 2DVAR grid is as regular as possible;
2. The new 2DVAR correctly interpolates irregularly spaced observations to the 2DVAR grid.

ASCAT data were processed for January 2015 from L2A BUFR data (ASCAT-25) and L1B full resolution data (other products). When compared with collocated buoy winds, the new 2DVAR has no significant effect on ASCAT-25, ASCAT-coastal, and ASCAT-6.25, and leads to a small improvement for ASCAT-5.6. It makes little difference if processing starts from L1B full resolution data or L2B BUFR data.

The new 2DVAR performs slightly better than the old one and is more flexible to accommodate future scatterometer processing. It is therefore implemented as standard.

Glossary

2DVAR	- Two-dimensional Variational Ambiguity Removal
ASCAT	- Advanced SCATterometer
AWDP	- ASCAT Wind Data Processor
ECMWF	- European Centre for Medium-Range Weather Forecasts
NWP	- Numerical Weather Prediction
WVC	- Wind Vector Cell

References

Vogelzang, J., and A. Stoffelen, 2017.
Developments in ASCAT wind ambiguity removal. NWP SAF Technical Report NWPSAF-KN-TR-026. Download from www.nwpsaf.eu/site/all-reports-publications.

Vogelzang, J., and A. Stoffelen, 2018.
Two-dimensional variational ambiguity removal (2DVAR), version 1.4. NWP SAF Technical Report NWPSAF-KN-TR-004. Download from www.nwpsaf.eu/site/all-reports-publications.